ELSEVIER

Composites: Part A 33 (2002) 1063–1072

composites
Part A: applied science and manufacturing

www.elsevier.com/locate/compositesa

Low-velocity impact-induced damage of continuous fiber-reinforced composite laminates. Part II. Verification and numerical investigation

C.F. Li[a,*], N. Hu[b], J.G. Cheng[a], H. Fukunaga[c], H. Sekine[c]

[a]*Department of Engineering Mechanics, Tsinghua University, Beijing 100084, People's Republic of China*
[b]*Department of Mechanical Engineering, The Johns Hopkins University, 3400 N. Charles Street, Baltimore, MD 21218, USA*
[c]*Department of Aeronautics and Space Engineering, Tohoku University, 01 Aramaki-aoba, Aoba-ku, Sendai 980-8579, Japan*

Received 5 February 2002; revised 14 June 2002; accepted 26 June 2002

Abstract

In Part I of the current work [this issue], we have developed a numerical model for simulating the process of low-velocity impact damage in composite laminates using the finite element method (FEM). This FEM model based on the Mindlin plate element can describe various impact-induced damages and their mutual effects. Some new and effective techniques have also been put forward in that paper, which can significantly increase the computational efficiency. In the current paper, i.e. Part II of the two-part series on the study of impact of composites, we focus on the following two aspects: (a) verification of our numerical model through the comparison with other researchers' results; (b) investigation of the impact-induced damage in the laminated plates using the present numerical model. For the first aspect, some previous experimental data have been adopted for comparison to validate the present numerical model. For the second, we have mainly studied the effects on the impact damage in detail in such aspects as the size of target plate, the boundary conditions of target plate, impact velocity, impactor mass, etc. From these computations, the understanding of the low-velocity impact damage in laminates can be improved.

Keywords: A. Polymer–matrix composites (PMCs); B. Fracture; B. Impact behavior; C. Finite element analysis (FEA)

1. Introduction

Many researchers have shown that the low-velocity transverse impact could cause various damages, such as matrix cracks, delamination and fiber breakage in fiber-reinforced polymer composite laminates. Such damages, especially delaminations, can cause significant reductions in the compressive strength of laminates and influence the reliability of structures. Hence, many previous studies [2–8] have been devoted to understanding the mechanisms and mechanics of the impact damage in the laminates and building up clear relationship between various parameters of impact events and those of damage extents (e.g. delamination size). However, there has been little work reported about the full and direct numerical simulation of the whole damage process. Actually, as stated previously [1], most of the current numerical approaches have roughly evaluated the delamination sizes using some simple empirical formulae [3,5,6] or simplified models with the aid of experimental information [7].

In Part I of the present work [1], which stems from our previous studies [9,10], we have developed an integrated and elaborate numerical model that can describe the various damages and their mutual effects. Obviously, a simple, reliable, and computationally efficient numerical model can greatly facilitate the study on this subject. Here, in Part II, we first verify our numerical model developed previously by comparison with some experimental results. Then, by using this numerical tool, the various aspects of impact phenomena have been effectively studied. The effects of various parameters on the impact process, especially on the impact-induced damages, have been investigated in such aspects as the size of target plate, the boundary conditions of target plate, impact velocity, impactor mass, etc. All these results can help us understand the impact damage process more comprehensively.

* Corresponding author. Tel.: +86-130-01917475; fax: +86-010-62781824.
E-mail address: lichenfeng99@mails.tsinghua.edu.cn (C.F. Li).

1359-835X/02/$ - see front matter
PII: S1359-835X(02)00078-7

2. Verification of the numerical model

It should be mentioned here that various aspects of the present numerical model have been verified in our previous researches [9,10]. Therefore, for simplicity, we directly employ some realistic experimental results to verify our model.

As stated previously [1], the present model deals with the cross-ply laminates, i.e. $0°/90°/0°$. The recent experimental work done by Collombet et al. [4] on the circular cross-ply laminates $0^n/90^m/0^n$, has been chosen for comparison. Three cases of stacking sequence are defined [4], i.e. Case 1: $n = 2$ and $m = 6$, Case 2: $n = 3$ and $m = 4$ and Case 3: $n = 4$ and $m = 2$. The parameters of the impactor are listed as: radius $r = 12.5 \times 10^{-3}$ m, effective density $\rho = 2.8113 \times 10^5$ kg/m^3, effective mass $m_s = 2.3$ kg, impact velocity $V = 4.85$ m/s, effective impact energy $e = 27.0$ J, Young's modulus $E = 210$ GPa and Poisson's ratio $\nu = 0.3$. We further define the following parameters used in the indentation law [1,11] as: $k = 2.583 \times 10^9$ N/m$^{1.5}$, $q = 2.0$, $\beta = 0.094$ and $\alpha_{cr} = 1.7 \times 10^{-4}$ m. The dimensions of the plate are: total thickness $t = 1.8 \times 10^{-3}$ m, and diameter of circular plate $d = 0.16$ m. The material properties of glass/epoxy composite are shown as: $\rho = 1.678 \times 10^3$ kg/m^3, $E_1 = 30.5$ GPa, $E_2 = E_3 = 6.9$ GPa, $\nu_{21} = 0.344$, $G_{12} = G_{13} = 4.65$ GPa, $G_{23} = 1.6$ GPa. As stated in Part I [1], several typical damage patterns, such as the fiber failure, matrix cracking, matrix crushing and delamination, have been considered. The material parameters used in the failure criteria of these damage patterns are defined as: $X_T = 700$ MPa, $Y_T = 100$ MPa, $Y_C = 237$ MPa, $S_{12} = 64$ MPa, $S_f = 120$ MPa, $S_{m23} = 200$ MPa, $S_{31} = 64$ MPa, $S_{123} = 86$ MPa and $G_C = 900$ J/m^2.

2.1. Verification of delamination size

For three stacking sequences, the comparisons of delamination sizes between experiment and numerical simulation are shown in Figs. 1–3. The delamination has been identified to occur on the interface between the middle 90° layers and bottom 0° layers [1]. From these figures, it can be found that the present numerical technique can produce very similar delamination shapes to those obtained in experiments. The main geometric features of the delamination, e.g. the peanut shape, can be captured. For further detailed comparisons, the data of three representative dimensions of delamination, i.e. the length, width and area of delamination as shown in Fig. 1, are plotted in Fig. 4. From this figure, it can be found that the length and width of delamination in numerical simulation agree very well with those practical ones. Also all delamination sizes predicted by numerical technique are a little higher although the errors are all within 10%. With the decrease in the thickness of middle 90° layers, the delamination area increases. There is also a representative geometric feature of delamination in Fig. 4. The length of delamination increases very quickly,

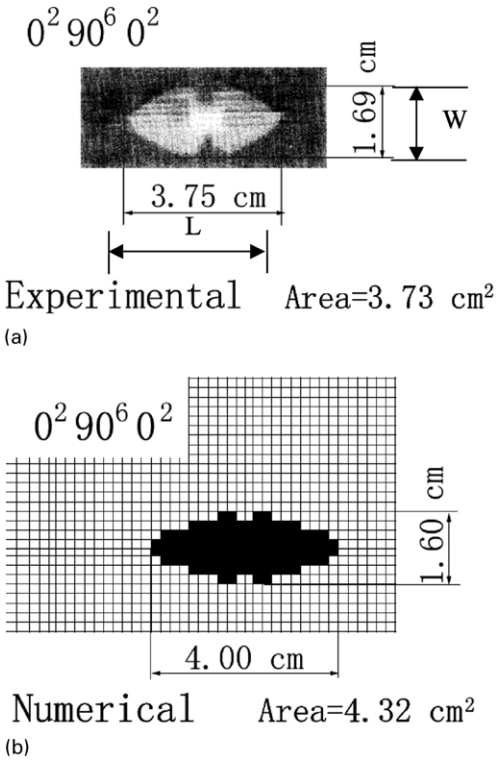

Fig. 1. Delamination in circular glass/epoxy cross-ply laminated plate $(0^2/90^6/0^2)$ impacted at 27 J. (a) Experimental result; (b) numerical result.

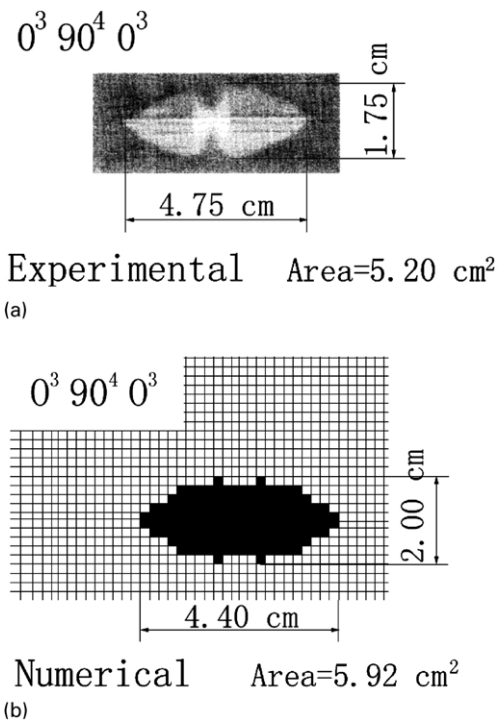

Fig. 2. Delamination in circular glass/epoxy cross-ply laminated plate $(0^3/90^4/0^3)$ impacted at 27 J. (a) Experimental result; (b) numerical result.

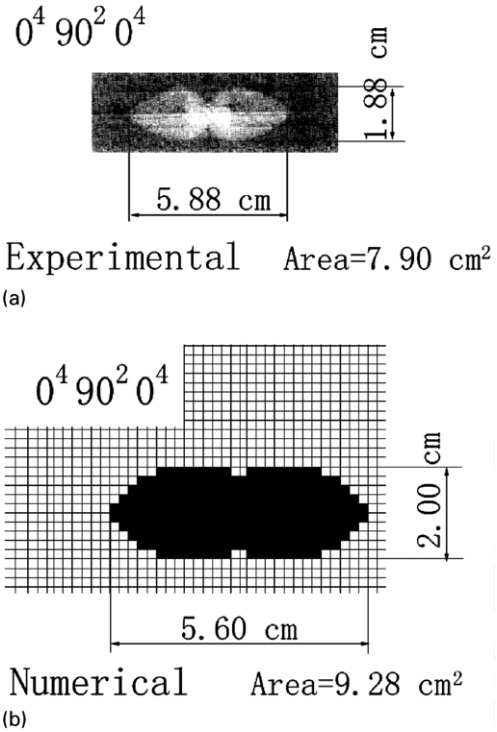

Fig. 3. Delamination in circular glass/epoxy cross-ply laminated plate $(0^4/90^2/0^4)$ impacted at 27 J. (a) Experimental result; (b) numerical result.

but the width of delamination increases slowly, as observed by other researchers [8].

2.2. Verification of matrix crack

The distributions of matrix cracks predicated by numerical simulation for impact energy of 27 J are shown in Fig. 5. The profiles of matrix cracks in Fig. 5 are similar to the sketch given in Ref. [4]. In our numerical model,

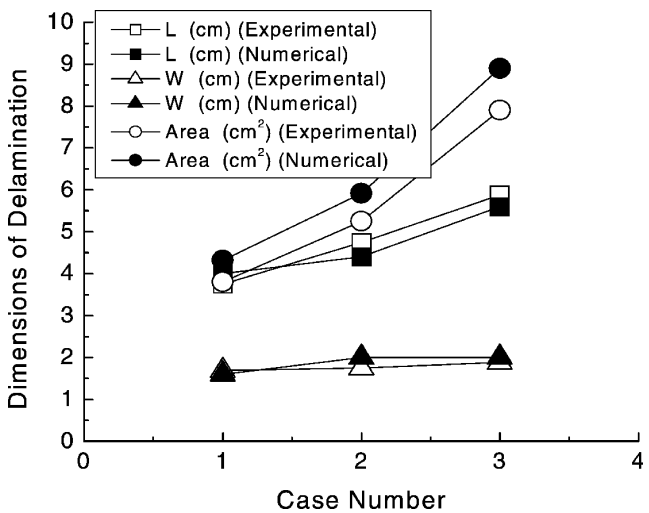

Fig. 4. Comparison between various dimensions of delamination obtained from experiment and those from numerical simulation for circular glass/epoxy cross-ply laminated plate impacted at 27 J corresponding to three different lay-ups.

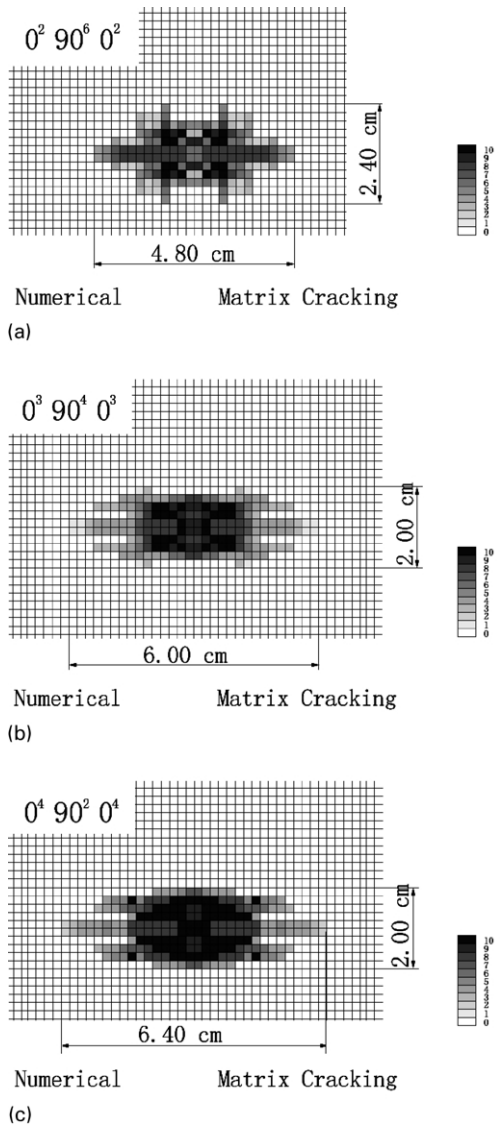

Fig. 5. Profiles of matrix cracks obtained from numerical simulation for circular glass/epoxy cross-ply laminated plate impacted at 27 J corresponding to three different lay-ups. (a) Numerical result of matrix cracks for $(0^2/90^6/0^2)$ under 27 J; (b) numerical result of matrix cracks for $(0^3/90^4/0^3)$ under 27 J; (c) numerical result of matrix cracks for $(0^4/90^2/0^4)$ under 27 J.

the matrix cracks can be predicted within various layers by using a kind of averaging technique [1]. In Fig. 5, the extent of matrix cracks is represented in gray scale. As the color becomes darker, more matrix cracks occur in more layers. From Fig. 5, it can be found that the profiles of distributions of matrix cracks are similar to the delamination shapes. Compared with the dimensions of delamination shown in Figs. 1–3, it can be found that the matrix cracks are distributed in larger areas, especially in the 0° direction. In two 0° layers, impacted and unimpacted, cracks are few and extended (bending cracks); whereas in 90° layer cracks (shear cracks) are numerous and short. From Case 1 $(0^2/90^6/0^2)$ to Case 2 $(0^3/90^4/0^3)$ and Case 3 $(0^4/90^2/0^4)$, with the decrease of the thickness of 90° layers,

these short matrix cracks in the 90° direction increase significantly since the stiffness in the 90° direction is reduced and the matrix cracks in these 90° middle layers can occur more easily. Also, the dimension of main cracks in the 0° direction tends to increase with the decrease of the thickness of 90° layers. All these phenomena have been identified in experiment [4].

2.3. Verification of force–time history and the central deflection

With regard to impact force and central deflection, the comparisons between the numerical and experimental results for three stacking sequences are shown in Figs. 6 and 7. It can be found from Fig. 6 that the force–time curves obtained from the proposed numerical model match well with the experimental ones, e.g. the period and peak value, except for some small fluctuations. The maximum deflection curves in Fig. 7 also give out a good map from numerical predication to experimental results. From Figs. 6 and 7 we can see that stacking sequence has no evident effect on time-dependent physical values, i.e. impact force and central deflection of the plates, as also shown in Ref. [4].

3. Numerical investigations

3.1. Numerical model

By using the current numerical model, we have studied the low-velocity impact phenomenon of continuous fiber-reinforced carbon/epoxy composite laminates. For cross-ply laminates $0^4/90^2/0^4$ with the thickness of single layer of 1.8×10^{-4} m, the material constants of composite are taken from Refs. [5,10], which are: $\rho = 1.58\times10^3$ kg/m^3, $E_1 =$ 139 GPa, $E_2 = E_3 = 9.4$ GPa, $\nu_{21} = 0.30905$, $G_{12} = G_{13} =$ 4.5 GPa, $G_{23} = 2.98$ GPa, $X_T = 2070$ MPa, $Y_T = 74$ MPa, $Y_C = 237$ MPa, $S_{12} = 64$ MPa, $S_f = 120$ MPa, $S_{m23} =$ 64 MPa, $S_{31} = 64$ MPa, $S_{l23} = 86$ MPa, $G_C = 240$ J/m^2. The parameters of the impactor are: radius $r = 6.35\times10^{-3}$ m, effective density $\rho = 2.5\times10^4$ kg/m^3, the effective mass is 0.0268 kg, $E = 210$ GPa and $\nu = 0.3$. The experimental parameters used in the indentation law between the ball and plates are taken from Ref. [11]: $k = 1.413\times10^9$ N/m$^{1.5}$, $q = 2.5$, $\beta = 0.094$ and $\alpha_{cr} = 1.7\times10^{-4}$ m. There are two kinds of boundary conditions, i.e. the simply-supported and clamped conditions and four kinds of plate sizes, i.e. lengths of plate equaling 0.2, 0.3, 0.4 and 0.5 m, taken into consideration. Furthermore, seven kinds of impact velocity ranging from 13 to 19 m/s are considered.

3.2. Numerical results

For a simply-supported plate with length of 0.2 m under the impact velocity of 19 m/s, Fig. 8 shows the delamination shape within the FEM mesh when $t = 2.2434\times10^{-4}$ s.

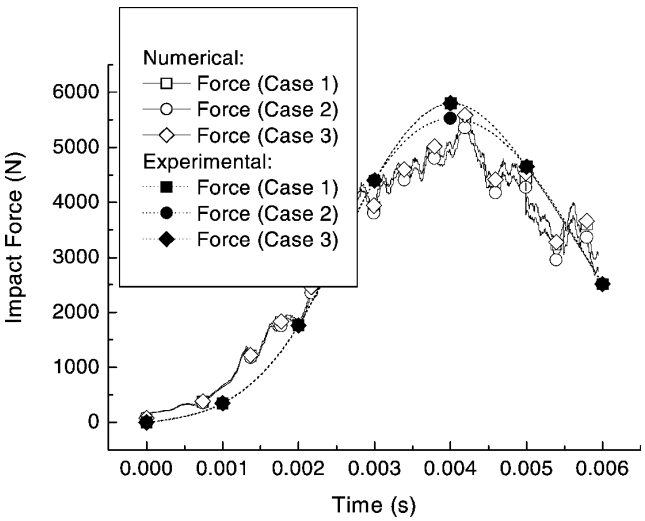

Fig. 6. Comparison of impact force history between numerical predication and experiment for circular glass/epoxy cross-ply laminated plate impacted at 27 J.

From this figure, it can be found that the peanut shape of delamination, which occurs on the interface of 90° layer and the bottom 0° layer, can be captured correctly by using our numerical model. Fig. 9 demonstrates the matrix cracks at this moment. Matrix cracks happen within the first six layers counting from bottom to top, including both 0 and 90° layers. Compared with the experimental photograph for the damages shown in Fig. 1 in Part I [1], it can be found that the present results obtained numerically can properly reflect the real situation. Compared with the matrix cracks shown in Fig. 5, the transverse cracks along the 90° direction in 90° layers in Fig. 9 are much less. The reason is that, on one hand, E_1/E_2 in the present computation is much higher than the previous case in Fig. 5, and in this case, the fibers in the 90° layers share much lower impact load compared with that carried out by the 90° layers in the previous case. On the other hand, the impact loads in the case of Fig. 5 are higher.

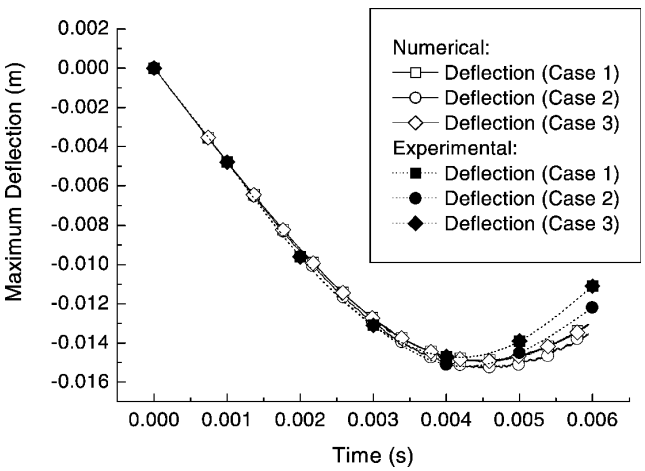

Fig. 7. Comparison of impact deflection history between numerical predication and experiment for circular glass/epoxy cross-ply laminated plate impacted at 27 J.

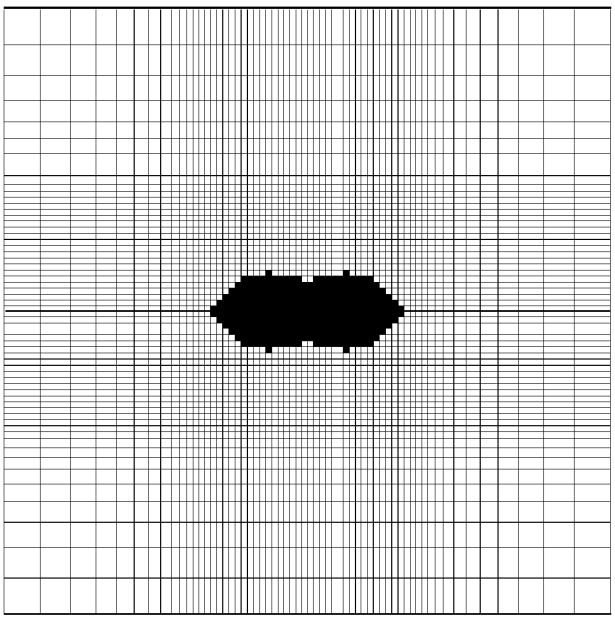

Fig. 8. Delamination shape at 90°/0° interface for a simply-supported plate with length of 0.2 m under the impact velocity of 19 m/s.

We can also identify some local matrix crush due to compression under the impactor. They occur within a very small area under the impactor and in the first two layers counting from top to bottom. No fiber breakage happens due to the low impact energy, i.e. maximum 4.8374 J.

Fig. 10 shows the history of impact force. From this figure, it can be found that the impact force increases very fast and reaches a local peak soon. After this peak, the impact force drops quickly, but insignificantly due to the first

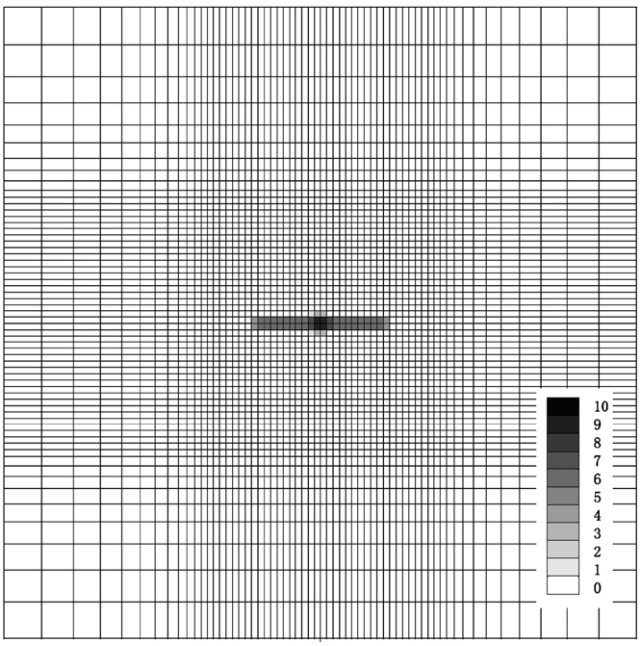

Fig. 9. Matrix cracks for a simply-supported plate with length of 0.2 m under the impact velocity of 19 m/s.

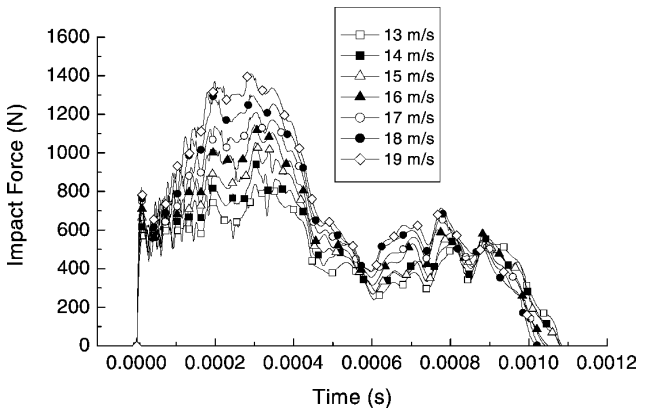

Fig. 10. Impact force of a simply-supported plate with a length of 0.2 m.

occurrence of the matrix cracks and the interface delamination they induced. With the extension of the matrix cracks and delamination, the impact force experiences an unstable and slow increase process. Of course, compared with the increasing process before damages occur, the slope of the increase of the impact force is much lower due to the reduction of the local and global stiffness of the laminates caused by various damages. After this unstable increase, the impact force undergoes a new higher and durative platform. Within this platform, the impact force reaches its highest peak. In usual cases, the various damages finish their extension procedure before the appearance of this highest peak in the impact force history. After this peak, the ball and plate start to separate from each other and the impact force comes through a decrease process. This typical procedure of impact force described above has been identified in many previous experiments [6]. Also, with the increase in the impact velocity, the impact force increases. Fig. 11 shows the central deflection of plates. In the case of 19 m/s impact velocity, the maximum deflection is already two times larger than the total thickness of the plate. Then, the plate obviously goes into the state of large deformation. This result testifies that the employment of the large deformation theory in our numerical model [1] is necessary. Fig. 12 shows the relationship between the occurrence time of

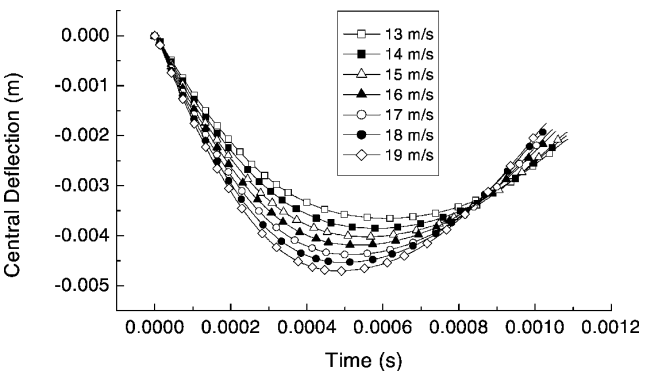

Fig. 11. Central deflection of a simply-supported plate with a length of 0.2 m.

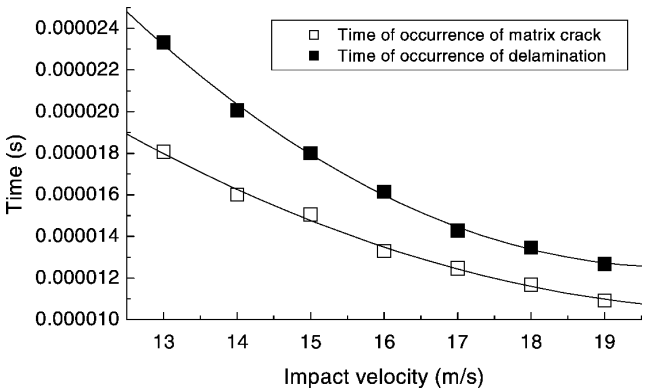

Fig. 12. Comparison of occurrence time between matrix crack and delamination for a simply-supported plate with a length of 0.2 m.

the matrix crack and delamination. From this figure, it can be found that matrix cracks always occur before delamination. As found in many previous experiments [2,3], the interface delamination is always triggered by the matrix cracks. This figure illustrates that our simulation result is reasonable in obtaining the correct mechanism of the impact damages. Actually, as stated in Ref. [5], some unreasonable simulation results have been obtained when using DYNA3D code, such as the earlier appearance of the delamination than the matrix cracks. Also, as shown in Fig. 12, with the increase of the impact velocity, both the matrix cracks and delamination appear earlier. By comparing Fig. 12 with Fig. 10, we can find that the first peak in the impact force history corresponds to the first occurrence of the matrix cracks. Before the moment of the first peak of the impact force, there is no matrix cracks and delamination extension except the assumed initial tiny delamination. Fig. 13(a) shows the extension history of the interface delamination. As a result of comparing with that in Fig. 10, all the delamination extensions finish before the appearance of the highest impact force. Also, with the increase of the impact velocity, the duration period of delamination extension becomes shorter and the delamination area increases. Fig. 13(b) shows the extension history of the matrix cracks. If the failure criterion for matrix cracks is satisfied within one specified element in one layer, this element area will be added to the total area of matrix cracks shown in Fig. 13(b). By comparison with those in Fig. 13(a) and (b), it can be found that the delamination area is more sensitive to the impact velocity than the area of matrix cracks. Fig. 14 shows the typical dimensions W and L of delamination defined in Fig. 1(a) in various models of the simply-supported and clamped plates, respectively. For simplicity, SS and CL represent the terms of 'simply-supported' and 'clamped' in this figure, respectively. The fitted curves from the isolated data obtained numerically are also plotted.

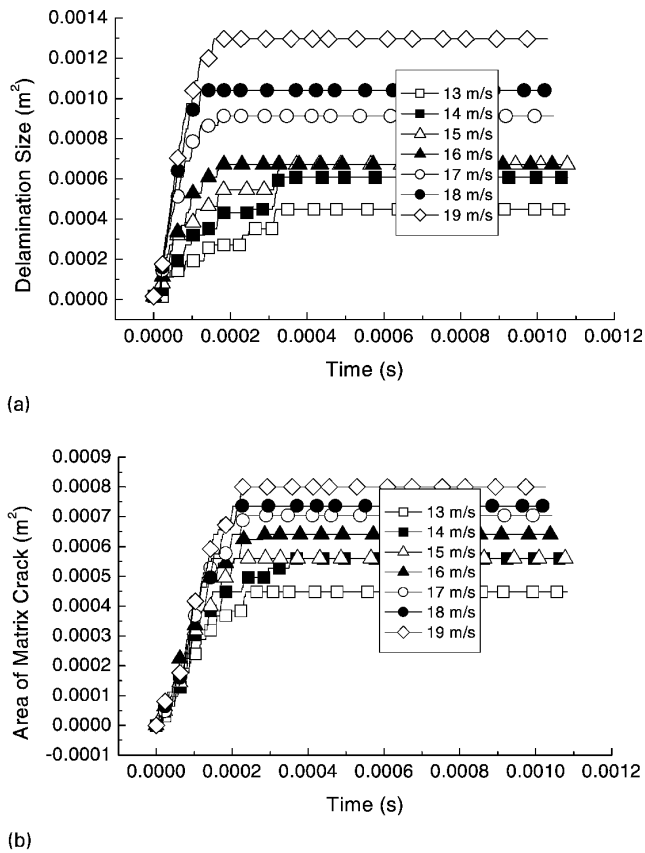

Fig. 13. Evolution history of delamination and matrix cracks for a simply-supported plate with a length of 0.2 m. (a) Delamination; (b) matrix crack.

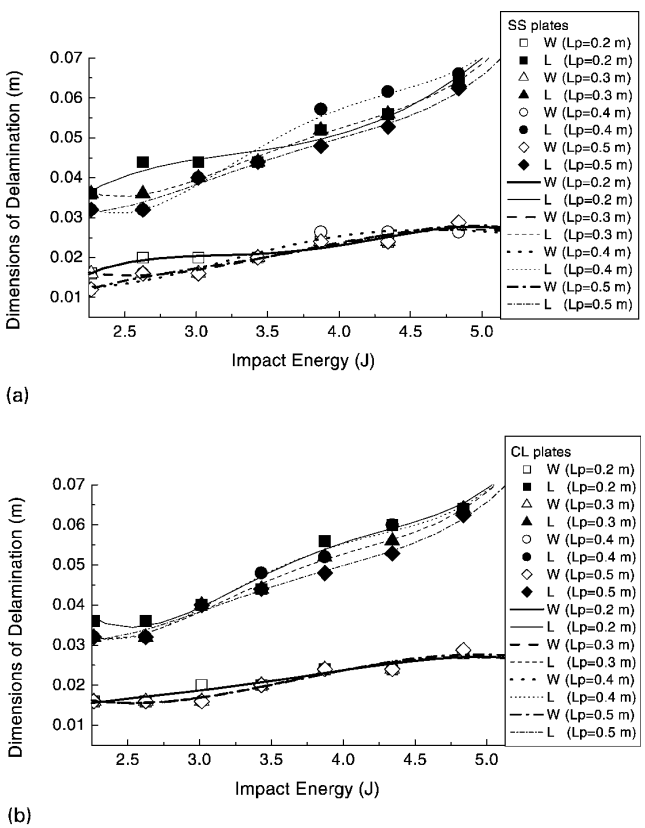

Fig. 14. Dimensions of delaminations (width W and length L) for simply-supported and clamped plates. (a) Simply-supported plate; (b) clamped plate.

In Fig. 14, Lp represents the length of the plate. From this figure, we can identify that L increases (i.e. the length of delamination) very quickly with the increase of the impact energy, however, W (i.e. the width of delamination) is insensitive to the impact energy. The relationship between two dimensions of delamination revealed in this figure has been identified in many previous experiments, e.g. Ref. [8]. Actually, this is one of most important geometric features for delaminations in composites.

3.3. Effect of plate size and boundary condition

Fig. 15 shows the effect of plate size on the maximum impact force, maximum central deflection and delamination size for plates of two kinds of boundary conditions. Fig. 15(a) shows that the maximum impact force decreases

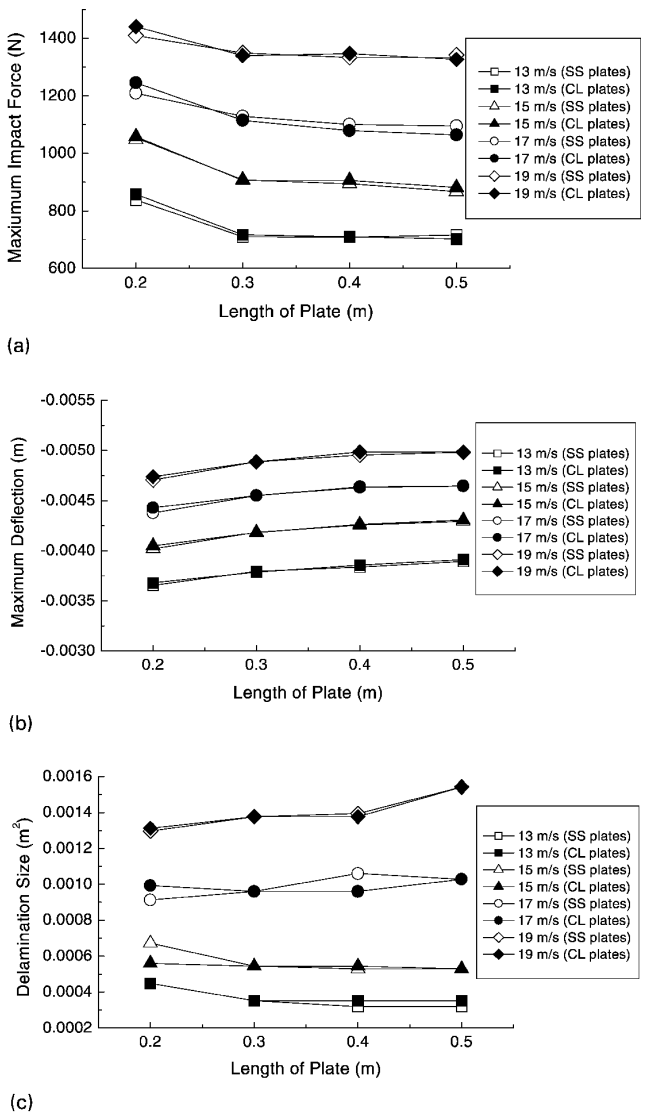

Fig. 15. Influence of plate size and boundary condition on maximum impact force, maximum central deflection and delamination size for simply-supported plates. (a) Maximum impact force; (b) maximum central deflection; (c) delamination size.

with the increase of the plate length due to the reduction of the global stiffness of plates. However, the effect of the plate size on the maximum impact force also decreases quickly with the increase of plate size. For example, when the plate length varies from 0.2 to 0.3 m, the maximum impact force drops significantly, but it drops very slowly when the plate length is larger than 0.3 m. Fig. 15(b) demonstrates that the maximum central deflection of plate increases with the increase of plate size. However, the tendency of this increase weakens gradually as the plate size becomes larger. Fig. 15(c) shows the effect of plate size on the delamination size. Surprisingly, from this figure, we found that the effect of plate size on the delamination size is not obvious when the impact velocity is low. However, when the impact velocity is high, e.g. larger than 17 m/s, there is an obvious tendency of increase in the delamination size with the increase of the plate size. To explain this phenomenon, we would first emphasize that the impact is basically a local phenomenon. When the impact velocity is low, the global deformation of plate is very small, and only the local area under the impactor deforms seriously. In this case, the delamination is basically dominated by the local deformation. Then the reduction of global stiffness of plate with the increase of plate size has very small influence on the impact damage process. However, when the impact velocity is large, the plate goes into very large deformation as shown in Fig. 11. The local deformation area becomes quite large and significant. In this case, the reduction of the global stiffness of plate may have more obvious influences on the local deformation under the impactor. Furthermore, the plate itself goes through a serious global bending deformation. Both the local deformation and global bending deformation dominates the delamination evolution in various stages. Then, in this case, when the plate size increases, the delamination size increases since the bending deformation becomes larger and the local deformation under the impactor becomes more drastic due to the reduction of global stiffness of plate. In general, however, from Fig. 15(c), it can be concluded that the effect of plate size on the final delamination size is not so significant. For example, for impact velocity equaling 19 m/s, the delamination size increases only around 10% although the plate length increases 2.5 times in size. The plate size has the similar effect on the matrix cracks.

Fig. 15(a) also shows the influence of boundary conditions on the maximum impact force. Inspection of this figure reveals that the effect of boundary conditions on the maximum impact force is very small. Only when the plate length is small, i.e. 0.2 m, a slight increase in the maximum impact force can be observed if the boundary condition is changed from the simply-supported to the clamped. When the plate size becomes larger, this effect becomes weak and obscure. Fig. 15(b) demonstrates that the effect of boundary conditions on the maximum central deflection is very small too. Fig. 15(c) shows the effect of

the boundary condition on the final delamination size. It can be found that there is no clear tendency to reveal this effect.

3.4. Effect of impactor mass

To study the influence of the impactor mass in the impact phenomenon, we set up four models for the simply-supported plates of length of 0.4 m. One of the models in Section 3.1, which possesses the impact energy 2.6264 J, the impact velocity 14 m/s and the effective mass 0.0268 kg, is selected as a reference point, and other models are set up by changing the mass and velocity of impactor, while keeping the impact energy constant. The influences of the impactor mass on the impact force history are shown in Fig. 16(a), from which, it can be found that the impactor mass has significant effect on the impact force history. With the increase of impact velocity and decrease of the impactor mass, the maximum impact force increases and the impact duration becomes shorter. Fig. 16(b) shows the effect of the impactor mass on the central deflection of plate. From this figure, we can find the maximum central deflection increases as the impactor mass increases. Fig. 16(c) demonstrates the extension history of delamination for various models. From this figure, it can be found that the delamination size increases significantly with the decrease of the impactor mass and the increase of the impact velocity. This increase of delamination size is more obvious for higher impact velocity range. Seemingly, the duration period of delamination extension becomes shorter with the decrease of the impactor mass and the increase of the impact velocity. Fig. 16(d) shows the extension history of matrix cracks. From this figure, we can get the similar conclusion as that obtained for the delamination. The only difference is that the increase of the area of matrix cracks is not as sensitive to the impact velocity range as that of the delamination. We have also analyzed another 4 models similar to the above four ones except for the plates of length of 0.2 m. The similar results have been obtained.

3.5. Prediction of delamination size

It is very important to find the relationship between the various impact parameters and the delamination size. Obviously, a reliable, clear and direct relationship can help people predict roughly the delamination size or damage extent easily and quickly.

Until now, there are various approaches to set up this relationship or map. The first and direct impact parameter

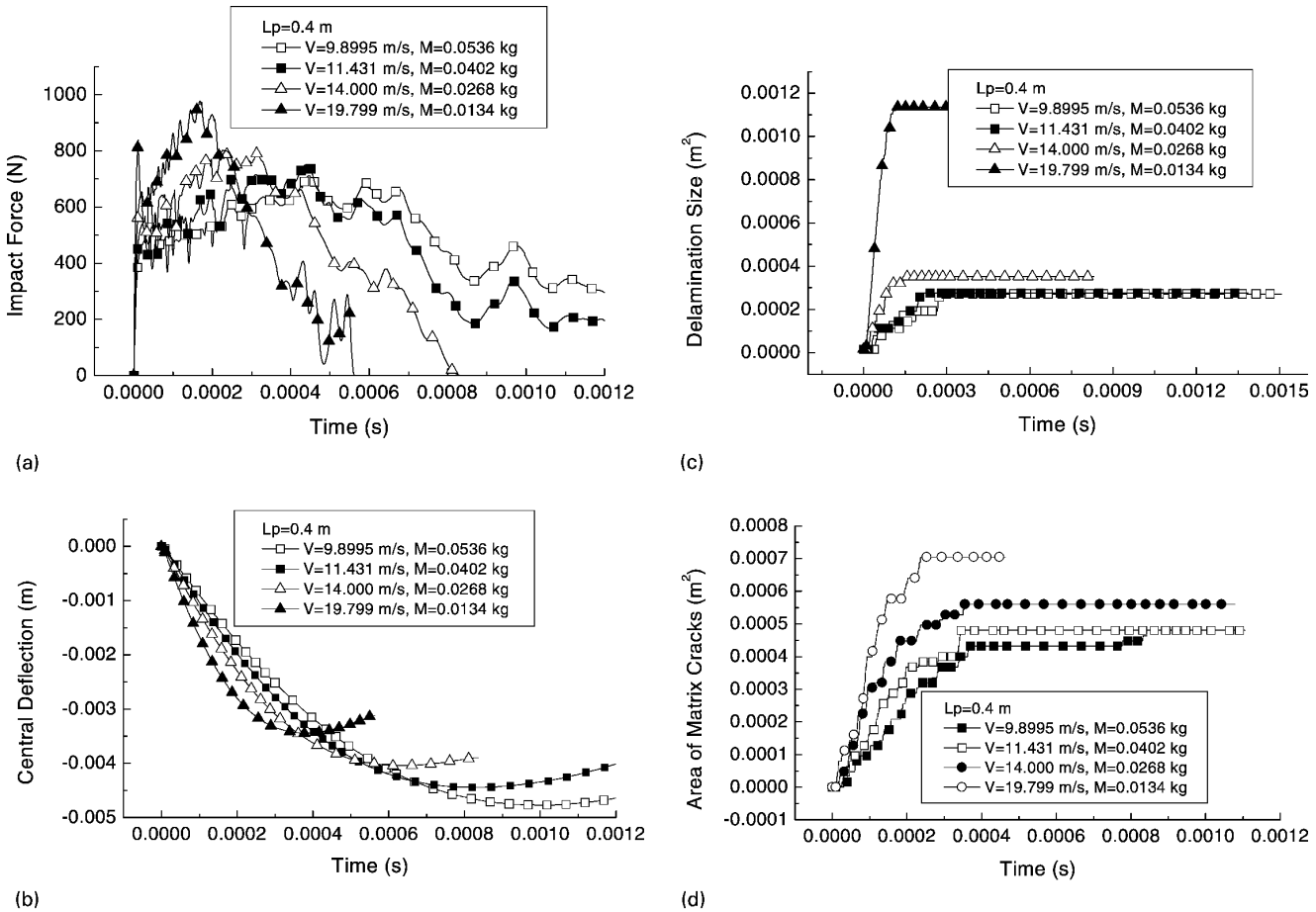

Fig. 16. Influence of impactor mass on impact force, central deflection, evolution history of delamination and matrix cracks (under the same impact energy). (a) Impact force; (b) central deflection; (c) evolution history of delamination; (d) evolution history of matrix cracks.

is the impact or incident energy. Before, many studies have been carried out to clarify the relationship between the impact energy and delamination size. Such kind of study is also performed here with the results shown in Fig. 17(a). The first eight sets of data in this figure are obtained from the impactor data stated in Section 3.1 where the impactor mass keeps constant. In this case, it can be found that the delamination size is correlated with the impactor energy in a very good linear relationship. The last two sets of data in this figure are those obtained from the impact data stated in Section 3.4, where the impact energy remains constant, while both the mass and impact velocity of impactor are changed. Of course, in this case, although the same impact energy is used, the delamination sizes are completely different as stated in Section 3.4. Moreover, Davies and Zhang [6] have reported that the increase of plate thickness can also cause the maps of impact energy versus delamination size to become increasingly more chaotic. So taking impact energy as the parameter to predicate the delamination size is confined in a small area, in which there are only variations of plate size and boundary conditions. If the impactor or the plate thickness is changed, the relevance with the delamination size becomes unclear.

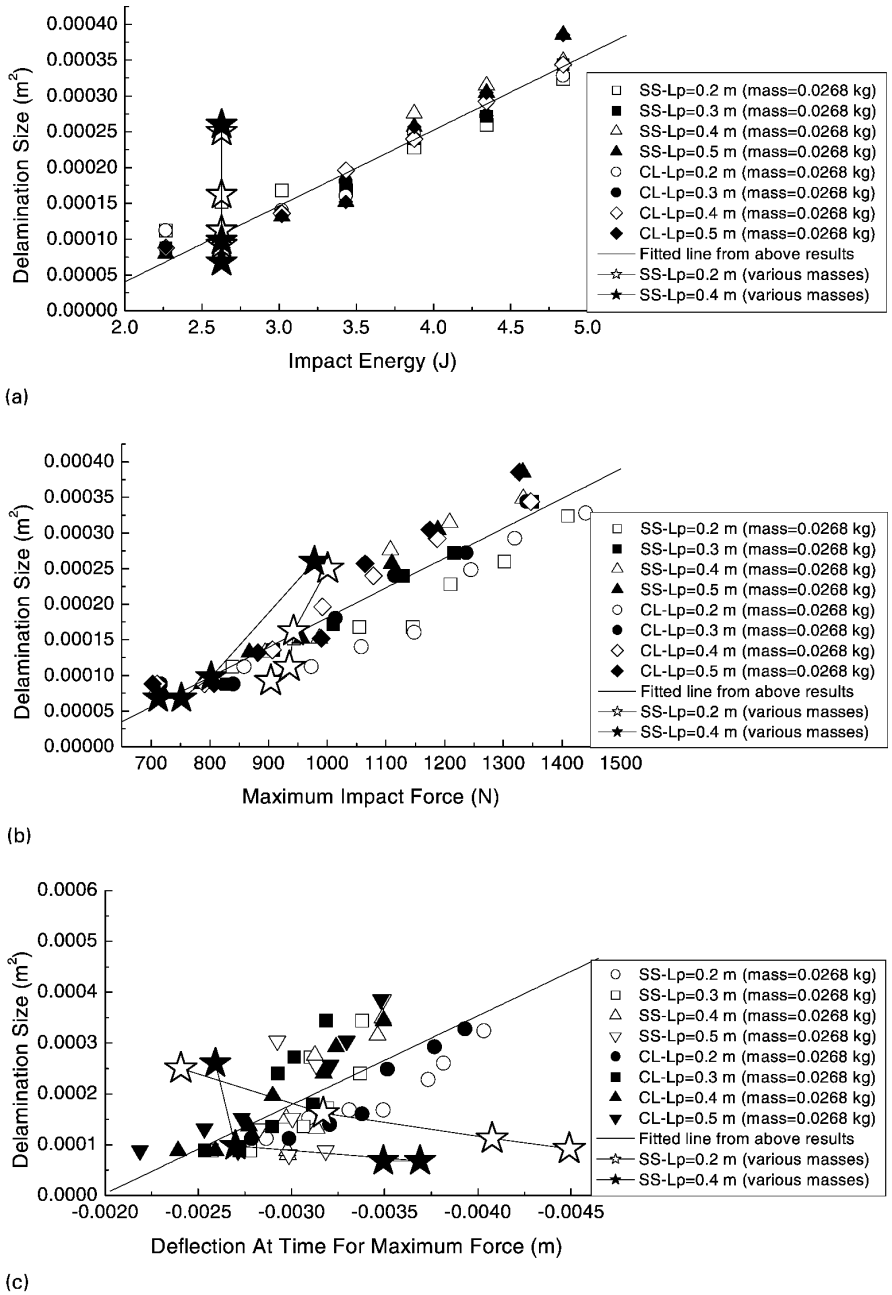

Fig. 17. Prediction of delamination size by various parameters. (a) Impact energy versus delamination size; (b) maximum impact force versus delamination size; (c) maximum central deflection versus delamination size.

The second parameter is the maximum impact force as used in Ref. [6]. Fig. 17(b) that shows the relationship between the maximum impact force and the delamination size. From this figure, we can find that the first eight sets of data can also create an acceptable linear relationship between the maximum impact force and the delamination size. For the last two sets of data with the variation of the impactor mass, the slope has a little change for plates of two lengths. It means that it may be difficult to create an accurate relationship to predict the delamination size only by using the maximum impact force. Other parameters, such as the impactor mass, should also be considered. However, these two last sets of data are still located quite near the fitted linear line. The maximum force is an approximately acceptable parameter to correlate itself to the delamination size.

Some researchers have also used the central deflection of plate when the maximum impact force occurs as an impact parameter to set up the relationship with the delamination size. Fig. 17(c) shows this relationship. From this figure, it can be found that the first eight sets of data become scattered and the linear relationship is not obvious. Furthermore, for the last two sets of data with the variation of impactor mass, we can find that slopes of the last two sets of data are completely different from those obtained from the first eight sets of data. In this case, with the increase of the central deflection of plates when the maximum impact force occurs, the delamination sizes even decrease. By checking Fig. 16(b), we can find that the maximum central deflection decreases with the decrease of the impactor mass and increase of the impact velocity. However, in this case, the delamination sizes increases as shown in Fig. 16(c).

4. Conclusions

In this paper, we first verified our previous FEM model based on the 9-node Mindlin plate element for directly simulating the low-velocity impact-induced damage in laminated plates [1]. It was found that this numerical model can capture the main features of impact phenomenon and reasonably predict various damages. Furthermore, various aspects of low-velocity impact of composites have been studied by using this model. From the numerical results, the following conclusions have been reached.

With the increase of plate size, the maximum impact force decreases, but the maximum central deflection increase. The influence of plate size on the delamination size is not obvious. Only when the impact velocity is comparatively high, the larger plate size will lead to a larger delamination size. The influence of the boundary condition on the maximum impact force, maximum central deflection and delamination size is very small. However, the impactor mass has very significant effects on the impact process. Under the condition of identical impact energy, with the decrease of mass and increase of impact velocity, the maximum impact force increases and the impact period becomes shorter. Both delamination size and the area of matrix cracks increase in this case. However, the maximum central deflection becomes smaller. When the plate size and boundary conditions change, the map of impact energy versus delamination area is clear. However, when the plate thickness and the impactor mass change, this relevance between the impact energy and delamination size becomes chaotic and unclear. It is unsuitable to use the deflection, which corresponds to the maximum impact force to predict the delamination size. The maximum force can be used to predict delamination size most effectively, except for a little dispersion of the data.

Acknowledgements

We would like to thank Prof. W.M. Zheng for his help. Computer systems used include the 144-node TS108 cluster system at Tsinghua University, and SW I system at Beijing High Performance Computer Center. Some authors were supported by the Natural Science Foundation of China under Grant 59875045 and by Basic Research Foundation of Tsinghua University under Grant JC200020.

References

[1] Li CF, Hu N, Yin YJ, Sekine H, Fukunaga H. Low-velocity impact-induced damage of continuous fiber-reinforced composite laminates. Part I. An FEM numerical model. Compos Part A 2002;33(8):1053–60.
[2] Choi HY, Wu HY, Chang FK. A new approach toward understanding damage mechanisms and mechanics of laminated composites due to low-velocity impact. Part II. Analysis. J Compos Mater 1991;25:1012–38.
[3] Choi HY, Chang FK. A model for predicting damage in graphite/epoxy laminated composites resulting from low-velocity point impact. J Compos Mater 1992;26:2134–69.
[4] Collombet F, Lalbin X, Lataillade JL. Impact behavior of laminated composites: physical basis finite element analysis. Compos Sci Technol 1998;58:463–78.
[5] Hou JP, Petrinic N, Ruiz C, Hallett SR. Prediction of impact damage in composite plates. Compos Sci Technol 2000;60:273–81.
[6] Davies GAO, Zhang X. Impact damage prediction in carbon composite structures. Int J Impact Engng 1995;16:149–70.
[7] Zheng S, Sun CT. A double-plate finite element model for the impact-induced delamination problem. Compos Sci Technol 1995;53:111–8.
[8] Wang H, Vu-Khanh T. Fracture mechanics and mechanisms of impact-induced delamination in laminated composites. J Compos Mater 1995;29:156–78.
[9] Sekine H, Hu N, Natsume T, Fukunaga H. Low-velocity impact response analysis of composite laminate with a delamination. Mech Compos Mater Struct 1998;5:257–78.
[10] Hu N, Sekine H, Fukunaga H, Yao ZH. Impact analysis of composite laminates with multiple delaminations. Int J Impact Engng 1999;22:633–48.
[11] Tan TM, Sun CT. Wave propagation in graphite/epoxy laminates due to impact. J Appl Mech 1985;52:6–12.